JAST, Vol. 3, No. 2, pp 61–66

JAST
Journal of Aerospace Science and Technology

Flutter Analysis of a Low Aspect Ratio Swept-Back Trapezoidal Wing at Low Subsonic Flow

S. Shokrollahi[1], H. Gerami[2], F. Bakhtiari-Nejad[3]

A linear, aeroelastic analysis of a low aspect ratio swept back trapezoidal wing modeled as a cantilever plate is presented. An analytical and numerical formulation for both the aerodynamic forcing and structural response of the wing was developed. The analytical model uses a three dimensional time domain vortex lattice aerodynamic method. A Rayleigh-Ritz approach has been used to transfer equations into a modal domain in order to solve equations of motion. The theoretical results are consistent with numerical results for low aspect ratio rectangular wings and experimental data reported by other investigators for delta wings.

INTRODUCTION

Mathematical models of wings based on equivalent plate representation combined with global Ritz analysis techniques have been used for basic studies in aeroelasticity and aeroelastic optimization for a long time. For structural analysis, the finite element Analysis (FEA) is widely used because of its generality, versatility and reliability. FEA is also the method of choice in situations where detailed results in the vicinity of local discontinuities such as holes, abrupt dimension variations, etc. are needed. This is accomplished by refinement of the mesh near the zone of interest. But a wide application of detailed FEA at the late conceptual design stage or in the early preliminary design stage still faces some major obstacles. First, the preparation time for a FEA model data may be prohibitive, especially when there is little carryover from design to design. Second, for complex structures a detailed FEA needs huge amount of CPU time and computation capacity, which incurs costs soaring. In view of this situation, equivalent continuum models are often used to simulate complex structures for the purpose of obtaining global solutions in the early design stages. This idea is reasonable as long as the complex structure behaves physically in a close manner to the continuum model used and only global quantities of the response are of concern. In the area of analyzing aeronautical wing structures, a number of studies have been conducted on using equivalent continuum models to represent simple box wings composed of laminated or anisotropic materials, and they have yielded accurate results for the specific problems studied.

Flutter and limit cycle oscillation characteristics of cantilevered low-aspect ratio, rectangular and delta wing models in low subsonic flow speeds have recently been studied. Hopkins and Dowell [1] as well as Weiliang and Dowell [2] studied the limit cycle oscillations of rectangular plates with three free edges while cantilevered on the forth side. The panel structure was of low aspect ratio and subject to quasisteady supersonic flow over one or both surfaces, a static temperature differential between the panel and its structural support, and a static pressure differential between the upper and lower surfaces of the panel. Their results provided good physical understanding of the flutter and limit cycle oscillation characteristics for such plates in a high-Mach-number supersonic flow. Deman Tang and Dowell [3,4] investigated limit cycle oscillations of cantilevered rectangular and delta plates at low subsonic flows. Their analysis included the vortex lattice theory in reduced-ordered aerodynamic model

1. *Assistant Professor, Department of Aerospace Engineering, Malek.e.Ashtar University of Technology, Tehran, Iran, E-mail: s_shokrollahi@yahoo.com*
2. *Research Associate, Structural Design Division, Department of Aerospace Engineering, Malek.e.Ashtar University of Technology, Tehran, Iran.*
3. *Professor, Department of Mechanical Engineering, Amirkabir University of Technology, Tehran, Iran.*

form that has been successfully applied to determine the nonlinear limit cycle oscillations of a cantilever plate model of a wing with a geometric structural nonlinearity. They also investigated the effect of a steady angle of attack on both the flutter instability boundary and the limit cycle oscillations. Bakhtiari-Nejad and Shokrollahi studied aeroelastic eigenanalysis of a cantilever plate in low subsonic flow to predict flutter onset [5]. The effect of local forcing functions on the response of a rectangular cantilevered plate at low subsonic flow was also studied by Bakhtiari-Nejad et.al. [6]. The piezoelectric actuators were used to model the local forcing functions and the effect of their position on flutter suppression were investigated. The theoretical and experimental results have provided good physical understanding of the relevant phenomena.

In the present paper, a three dimensional time domain vortex lattice aerodynamic model is used to investigate the flutter characteristics of low aspect ratio swept back trapezoidal wings at low subsonic flow. The effect of wing geometrical characteristics such as taper ratio, sweep angle and aspect ratio are also investigated.

Theoretical Development

A plan view schematic of the wing-plate geometry with a three dimensional vortex lattice model of unsteady flow is shown in Figure 1. The aeroelastic structure/fluid state-space equations are described as follows.

TRAPEZOIDAL WING STRUCTURAL MODEL

The swept back trapezoidal wing model under consideration is assumed to behave as a thin plate of uniform mass and stiffness. The following general formulation allows the treatment of a whole family of rectilinear wings of arbitrary constant taper and aspect ratios through the use of transformation to the normalized beam mode coordinates. With standard aerodynamic nomenclature, wing taper ratio (TR) is defined as a ratio of the wing tip chord, c_t to the root chord c_r, and aspect ratio (AR) is defined in terms of root chord, semi span (L), and taper ratio as,

$$AR = \frac{Span^2}{WingArea} = \frac{4}{1+TR}\left(\frac{L}{c_r}\right). \tag{1}$$

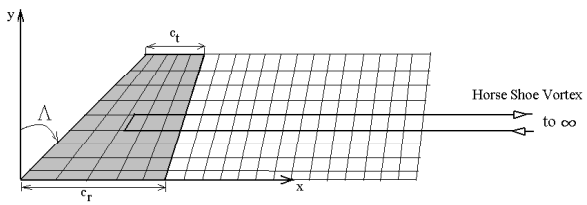

Figure 1. Aeroelastic model of a swept back trapezoidal cantilever plate

To facilitate the use of clamped-free and free-free beam functions for approximating mode shapes of the plate and any wing fittings, the preceding description can be mapped to a unit square domain referred as the normalized beam coordinates. The transformations given by Eq. (2), map any point from physical coordinates on the wing to the normalized beam coordinates.

$$\xi = \frac{x/c_r - \frac{AR}{4}(1+TR)\tan\lambda(y/L)}{1-(1-TR)y/L}, \quad \eta = y/L, \tag{2}$$

and a corresponding pair of inverse transformations given by Eq. (3) map them back,

$$x/c_r = [1-(1-TR)\eta]\xi + \frac{AR}{4}(1+TR)\tan\lambda\eta, \; y/L = \eta. \tag{3}$$

For this study, a swept back trapezoidal wing is considered, as shown in Figure 1. In accordance with the Ritz method, Eq. (4) gives the total transverse displacement at any point on the wing, which can be expressed as a time-dependent weighted sum of assumed spatial mode shape functions.

$$w(x,y,t) = \sum_{1}^{Nm}\sum_{1}^{Nn} R_{mn}(x,y)q_{mn}(t). \tag{4}$$

These spatial shape functions as given in Eq. (5) are in turn products of assumed beam modes in the chordwise and spanwise directions.

$$R_{mn}(x,y) = \psi_m(\xi(x,y)) \times \phi_n(\eta(x,y)), \tag{5}$$

where $\psi_m(\xi)$ given by Eq. (6) are the one-dimensional free-free beam modes in the chord wise direction of the plate in the following forms,

$$\psi_1(\xi) = 1,$$

$$\psi_2(\xi) = \sqrt{3}(1-2\xi),$$

$$\psi_m(\xi) = [\cos(\alpha_m x) + \cosh(\alpha_m x)] - \left[\frac{\cos(\alpha_m) - \cosh(\alpha_m)}{\sin(\alpha_m) - \sinh(\alpha_m)}\right] \times [\sin(\alpha_m x) + \sinh(\alpha_m x)], \quad m \geq 3 \tag{6}$$

and $\phi_n(\eta)$ given by Eq. (7), are the one-dimensional clamped-free beam modes in the span wise direction.

$$\phi_n(\eta) = -[\cos(\beta_n\eta) - \cosh(\beta_n\eta)] - \left[\frac{\sin(\beta_n) - \sinh(\beta_n)}{\cos(\beta_n) + \cosh(\beta_n)}\right] \times [\sin(\beta_n\eta) - \sinh(\beta_n\eta)]. \tag{7}$$

These functions are orthonormal over the range $0 \leq \xi, \eta \leq 1$ and have associated wave numbers given in Table 1.

Table 1. Approximate spatial wave numbers for free-free and clamped –free beam modes

i	α_i	j	β_j
3	4.7300407	1	1.8751041
4	7.8532046	2	4.6940911
5	10.995608	3	7.8547574
≥ 6	$(\pi/2)(2i+1)$	≥ 4	$(\pi/2)(2j-1)$

TRANSVERSE EQUATIONS

The transverse equation is formed by substituting the kinetic and strain energy expressions into Lagrange's equation [7]. The nondimensional equation is

$$\sum_m \sum_n \left[A^{ij}_{mn}\ddot{q}_{mn}(\tau) + B^{ij}_{mn}q_{mn}(\tau)\right] + Q^{ij} = 0, \qquad (8)$$

where A^{ij} and B^{ij} are coefficient terms and Q^{ij} is the nondimensionalized generalized aerodynamic force which will be discussed in the next section.

AERODYNAMIC METHOD: VORTEX LATTICE MODEL

The flow about the cantilever trapezoidal plate is assumed to be incompressible, inviscid, and irrotational. Here we use an unsteady vortex lattice method to model this flow. A typical planar vortex lattice mesh for the three-dimensional flow is shown in Figure 1. The plate and wake are divided into a number of elements. Point vortices are placed on the plate and in the wake at the quarter chord of the elements. At the three-quarter chord of each plate element, a collocation point is placed for the downwash; i.e., we require the velocity induced by the discrete vortices to equal the downwash arising from the unsteady motion of the plate. Thus, the relationship will be

$$w_i^{t+1} = \sum_j^{kmm} K_{ij}\Gamma_j^{t+1}, \qquad i = 1, \ldots, kmm \qquad (9)$$

where w_i^{t+1} is the downwash at the ith collocation point at time step t+1, Γ_j is the strength of the jth vortex, K $_{ij}$ is an aerodynamic kernel function that is given in Reference 9 and kmm is the total number of vortices on both the plate and wake in x direction.

As described by Bakhtiari-Nejad et al [5], there are three sets of equations in the wake. Eq. (10) gives the first vortex in the wake at the step time of t+1.

$$\Gamma_{km+1}^{t+1} = -\sum_j^{km}(\Gamma_j^{t+1} - \Gamma_j^t), \qquad (10)$$

where km is the number of vortex elements on plate in x direction. Once the vorticity has been shed into the wake, it convects in the wake at U speed. From the second vortex point to the last two vortex points in the wake for the special case where $\Delta t = \Delta x/U$ this convection is described numerically by Eq.(11).

$$\Gamma_i^{t+1} = \Gamma_{i-1}^t, \quad i = km+2, ..., (kmm-1)*kn \qquad (11)$$

where kn is the number of vortex elements on plate in y direction. At the last vortex point in the wake, Eq. (12) drives the relationship for the vortex distribution:

$$\Gamma_i^{t+1} = \Gamma_{i-1}^t + \alpha\Gamma_i^t, \qquad i = kn \qquad (12)$$

where α is a relaxation factor used for considering the effect of the omitted part of the wake, usually having values of 0.95< α<1.0.

Putting together Eqs. (9) to (12) gives an aerodynamic matrix equation of,

$$A\Gamma^{t+1} + B\Gamma^t = w^{t+1}, \qquad (13)$$

where A and B are aerodynamic coefficient matrices. From the fundamental aerodynamic theory, we can obtain the pressure distribution on the plate at the jth point in terms of the vortex strength as:

$$\Delta\bar{p}_j = \frac{1}{\Delta\xi}\left[\frac{E(\eta)(\Gamma_j^t + \Gamma_j^{t+1})}{2} + \sum_{i=1}^{j}(\Gamma_i^{t+1} - \Gamma_i^t)\right], \qquad (14)$$

Here $E(\eta)$ is a component of Jacobian matrix and is defined by:

$$E(\eta) = \frac{1}{1-(1-TR)\eta},$$

and the aerodynamic generalized force is calculated from:

$$Q^{ij} = \frac{\rho_\infty U^2 c_r^4}{Dh}\int_0^1\int_0^1 \Delta p\phi_i(\xi)\psi_j(\eta)\frac{d\xi d\eta}{E(\eta)}.$$

AEROELASTIC STATE SPACE MODEL:

In this stage we can combine structural dynamics response with aerodynamic equations to obtain the aeroelastic model. Consider a discrete-time history of plate motion q(t), with a constant sampling time step Δt. The sampled version of q(t) is then described by:

$$q = \frac{(q^{t+1} + q^t)}{2}, \qquad (15)$$

And the velocity of this discrete-time series is defined by:

$$\dot{q} = \frac{(q^{t+1} - q^t)}{\Delta t}. \qquad (16)$$

The structural dynamic, equation (8) can be reconstituted as a state-space equation in discrete-time form. It is given by:

$$D_2\theta^{t+1} + D_1\theta^t + C_2\Gamma^{t+1} + C_1\Gamma^t = 0, \qquad (17)$$

where the vector θ is the state of the plate, $\{\theta\} = \{\dot{q}, q\}$, and D_1 and D_2 are matrices describing the plate structural behavior. C_1 and C_2 are matrices describing the vortex element behavior on the plate itself. There is a linear relationship between the downwash w at the collocation points and plate response θ. It is defined by:

$$w = E\theta. \tag{18}$$

Thus, combining Eqs.(13), (17), and (18), we obtain the aeroelastic state-space model in the matrix form:

$$\begin{bmatrix} A & -E \\ C_2 & D_2 \end{bmatrix} \begin{Bmatrix} \Gamma \\ \theta \end{Bmatrix}^{t+1} + \begin{bmatrix} B & 0 \\ C_1 & D_1 \end{bmatrix} \begin{Bmatrix} \Gamma \\ \theta \end{Bmatrix}^{t} = \begin{Bmatrix} 0 \\ 0 \end{Bmatrix}^{t+\frac{1}{2}} \tag{19}$$

We refer to Eq.(19) as the complete discrete time fluid/structure model. The eigenvalue solution of this discrete time model determines the stability of the aeroelastic system in terms of eigenvalues, z_i. If any of the eigenvalues have magnitudes greater than unity, then the system is unstable. In principle, one could find the eigenvalues of eq.(19) directly. However, for most aeroelastic calculations, one must compute the eigenvalues of the system as a function of some parameters, such as the variation of reduced velocity.

NUMERICAL RESULTS

Various types of swept back trapezoidal cantilever plate models of varying aspect and taper ratios were considered. The models are taken to be an aluminum alloy plate of constant thickness with aspect ratios of AR =L/c =2.-10 and taper ratios of TR =0.5, 0.75 and 1. The wing root chord cr = 0.365 is fixed. The plate thickness is h = 0.001 m, and Poisson's ratio is ν = 0.3. For the basic case, the plate was modeled using 50 vortex elements, i.e., km =10 and kn =5. The wake

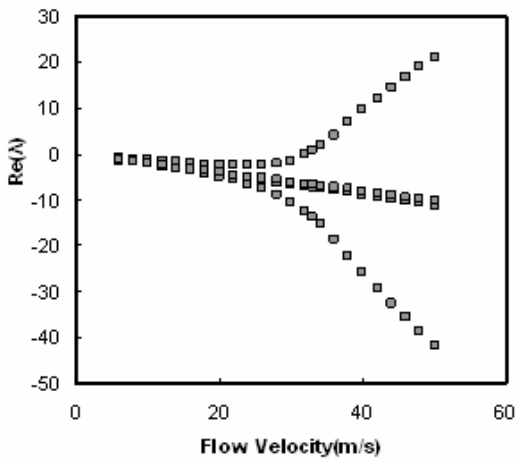

Figure 2. Eigenvalue Solution for Aeroelastic model, For Sweep angle of Leading Edge =30.

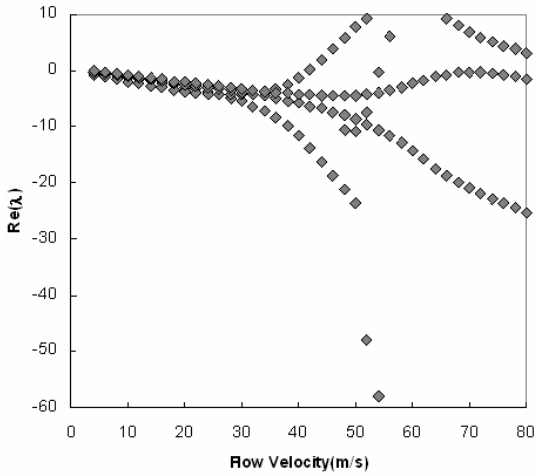

Figure 3. Eigenvalue Solution for Aeroelastic model, For Sweep angle of Leading Edge=0.

was modeled using 150 vortex elements, i.e., kmm =40. The total number of vortex elements (or aerodynamic degrees of freedom) is 200. The vortex relaxation factor was taken to be $\alpha = 0.992$.

STABILITY OF THE AEROELASTIC MODEL

The aeroelastic eigenvalue solutions of linear model determine the stability of the system. The discrete-time eigenvalues z_i are related to continuous-time eigenvalues λ_i by $z_i = \exp(\lambda_i \Delta t)$. When the real part of any eigenvalue, λ becomes positive, the entire system becomes unstable.

Figure 2 shows a typical graphical representation of the eigenanalysis in the form of real eigenvalues; Re(λ) vs. the flow velocity for Sweep angle of Leading Edge =30 degrees. There is an intersection of Re (λ) with the velocity axis at U_f = 32.1 m/s, which is the critical flutter velocity. From Figure 2 it is also found that in contrast to rectangular wings, for swept back wings, static instability (divergence) does not occur while the flutter velocity decreases by increasing the sweep angle.

Figure 3, in consistency with the results of References 3 and 5, shows graphical representation of the eigenanalysis in the form of real eigenvalues; Re(λ) vs. the flow velocity for sweep angle of leading edge=0 degrees (rectangular wing). In this case there are two intersections of Re(λ) with the velocity axis. One is $U_f = 42m/s$ for the critical flutter velocity with the corresponding flutter oscillatory frequency 76.8 rad/s. The other is $U_d = 54.3m/s$ for divergent velocity with zero oscillatory frequency. From Figures 3 and 4 it is found that the linear flutter motion is dominated by the coupling between the first two structural modes, i.e., the spanwise bending mode and rigid plunge and rotation modes in the chordwise direction.

The variation of flutter velocity vs. sweep angle, for various taper and aspect ratios is given in Figures 4 to 7. These figures show that, at all cases there is a minimum critical flutter velocity. For example, for AR =4.0 and TR = 0.5 minimum flutter velocity is nearly 33.8 m/s. Figures 4 to 7 also show that by increasing the TR from 0.5 to 1.0 for a given aspect ratio and sweep angle, the flutter velocity decreases. For example, with AR =4.0 and λ=30 deg the flutter velocity decreases from 34 to 17.35 m/s.

CONCLUDING REMARKS

A trapezoidal cantilever plate with 3 dimensional vortex lattice aerodynamic theory has been used to investigate the aeroelastic characteristics of a swept back trapezoidal wing in low subsonic flow. There are several parameters including sweep angle, taper ratio and aspect ratio that have considerable effects on aeroelastic behavior and characteristics of these wings. It is found that in contrast to rectangular wings, for swept back wings, static instability (divergence) does not occur while the flutter velocity decreases by increasing the sweep angle.

The results presented in this work are exactly consistent with numerical results for low aspect ratio rectangular wings and experimental data for delta wings reported by other investigators [3, 4,5,6,8]. This analysis can be used adequately for aircraft design procedures and estimation of the optimum aspect ratio, taper ratio, and sweep angle of an aircraft wing especially on conceptual design stages. The results of this paper are consistent with those of other investigators such as References 3 to 5, of which two cases are given here as Figures 2 and 10 for rectangular wings with sweep angle of 0 degrees and taper ratio of 1.

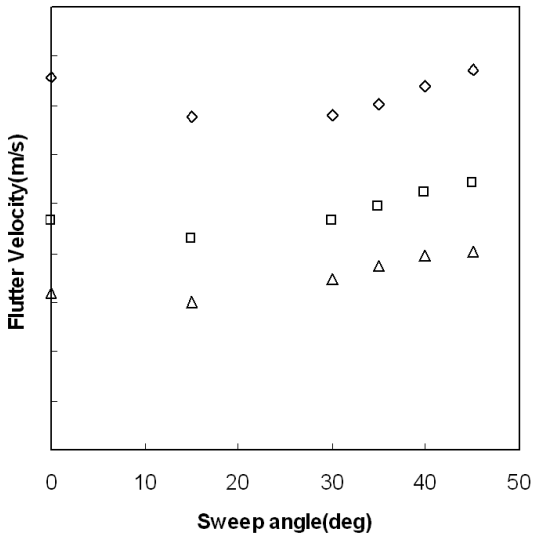

Figure 4. Flutter velocity.vs. Sweep Angle for AR=2, (□: TR= 0.5, ◇: TR=0.75, △: 1.0).

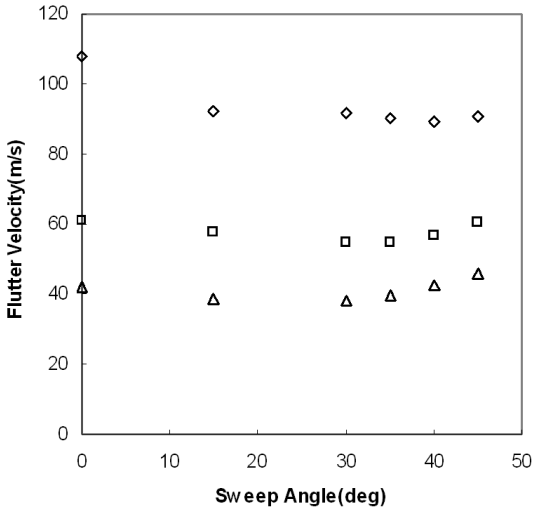

Figure 5. Flutter velocity.vs. Sweep Angle for AR=4, (□: TR= 0.5, ◇: TR=0.75, △: 1.0).

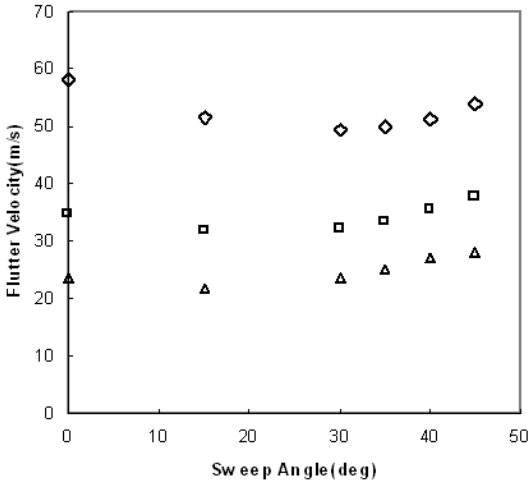

Figure 6. Flutter velocity.vs. Sweep Angle for AR=3, (□: TR= 0.5, ◇: TR=0.75, △: 1.0).

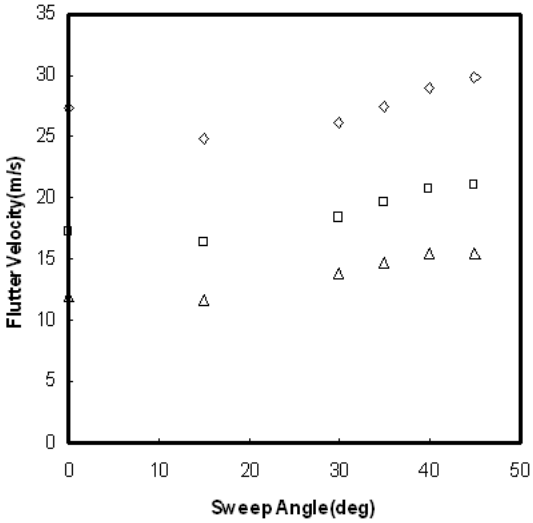

Figure 7. Flutter velocity.vs. Sweep Angle for AR=5, (□: TR= 0.5, ◇: TR=0.75, △: 1.0).

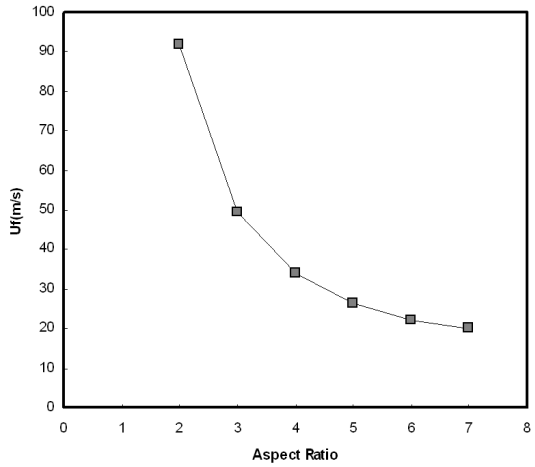

Figure 8. Flutter velocity.vs. Aspect Ratio for Sweep Angle of Leading Edge =30 and TR=0.5.

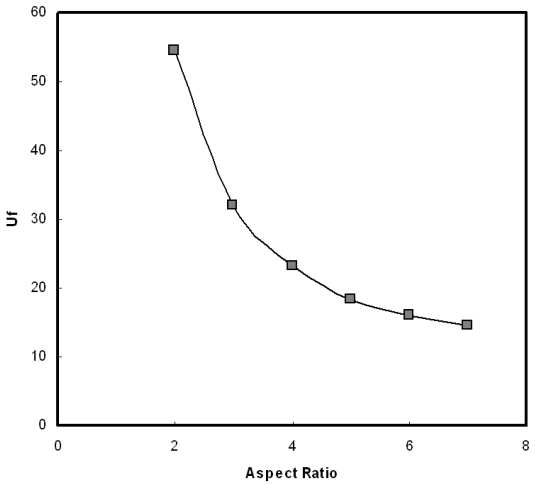

Figure 9. Flutter velocity.vs. Aspect Ratio for Sweep Angle of Leading Edge and TR =0.75.

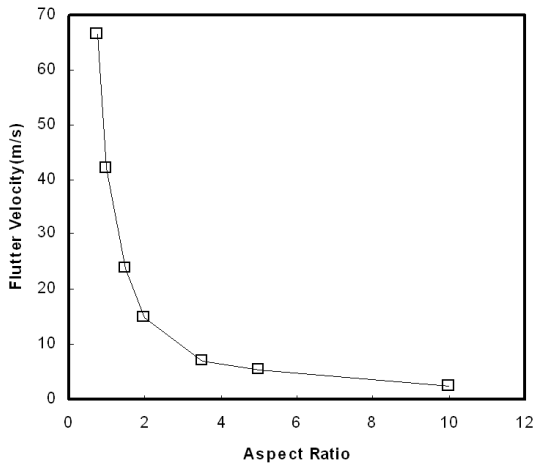

Figure 10. Flutter velocity.vs. Aspect Ratio for Sweep Angle of Leading Edge =0 and TR=1.

REFERENCES

1. Hopkins, M. A., and Dowell, , E.H., "Limited Amplitude panel flutter with a temperature Differential", proceeding of the AIAA/ASME /ASCE/AHS /ASC 35th structures, structural Dynamics, and Materials conference, AIAA, Washington, DC , PP 1343-1355(1994).
2. Weiliang, Y., and Dowell,E.H., "Limit cycle oscillation of a fluttering cantilever plate", *AIAA Journal*, **32**(12), PP 2426-2432(1994).
3. Deman Tang, Earl H. Dowell, and Kenneth C. Hall, "Limit Cycle Oscillations of a cantilevered Wing in Low Subsonic Flow ", *AIAA Journal*, **37**(3), PP 364-371(1999).
4. Tang, D.M., Henry, J.K., and Dowell, E. H., "Limit Cycle Oscillations of a delta Wing model in Low Subsonic Flow ", *AIAA Journal*, **37**(11), PP 1355-1362(1999).
5. Bakhtiari-Nejad,F., Shokrolahi,S., "Aerelastic Eigenanalysis of a Cantilever Plate in Low Subsonic Flow to Predict Flutter Onset", Proceeding of ISME 10th International conference of Mechanical Engineering, Tehran, Iran., (2002).
6. Bakhtiari-Nejad, F., Shokrollahi, S., Dardel, M., "Effect of Local Forcing Functions on Flutter Suppression of a Low Aspect Ratio Rectangular Cantilever Plate ", *ICSV9 2002*, (2002).
7. Dowell, E.H., "Aeroelasticity of plates and shells", Kluwer,Dordecht, The Netherlands, PP 35-49(1975).
8. Doggett, R.V., and Soistman. D. L., Jan., "Some Low-Speed Flutter Characteristics of Simple Low-Aspect-Ratio Delta Wing Models ", *NASA TM-101547*, (1989).
9. John. J.Bertin, and Michael. L. Smith, "Aerodynamics for Engineers", Second Edition, Prentice-Hall, International Editions , PP 271(1989).